Towards the personalization of 3D printed patches for cosmetic applications

Bom, Sara[1]; Ferreira, Marta[2]; Santos, Catarina[1,2,3]; Cláudio, Ricardo[1,2]; Pinto, Pedro[1,4]; Ribeiro, Helena Margarida[1], **Marto, Joana[1*]**

[1] Research Institute for Medicines (iMed.ULisboa), Faculty of Pharmacy, Universidade de Lisboa, Portugal; [2] EST Setúbal, CDP2T, Instituto Politécnico de Setúbal, Portugal; [3] CQE Instituto Superior Técnico, Universidade de Lisboa, Av. Rovisco Pais 1049-001, Lisboa, Portugal; [4] PhD Trials, Avenida Maria Helena Vieira da Silva, nº 24 A – 1750-182, Lisboa, Portugal.

* Joana Marques Marto, Research Institute for Medicines (iMed.ULisboa), Faculdade de Farmácia, Universidade de Lisboa, Avenida Professor Gama Pinto 1649-003 Lisboa, jmmarto@ff.ulisboa.pt

Abstract

Background: The production of cosmetic products by semi-solid extrusion 3D printing has been explored as a solution to personalize skincare products. Therefore, the main goal of this work was to develop an innovative and versatile gelatin-based 3D printed patch with controlled network topology for multipurpose cosmetic applications, such as anti-aging, and which can be easily personalized by changing print parameters.

Methods: 3-Layered gelatin-based patches with several infill patterns were printed in an extrusion-based 3D printer (Allevi2, USA), varying the line distance and the angles. Measurements of pore width were performed using the ImageJ® software and Visioscan® was used to record the topography. Afterwards, Visia-CR™ was employed as: i) biometric equipment to record the bioactive fluorescence; and, ii) 2D scanner for designing a personalized eye patch with controlled network topology.

Results: Gelatin-based patches with different degrees of porosity were successfully printed and showed good bioactives release modulation properties. As a proof-of-concept, an anti-aging purified tomato extract, IBR-TCLC®, was incorporated into the personalized eye patch. Topographic analysis showed that the printing accuracy and pore shape fidelity were not largely affected by this incorporation, reinforcing the versatility of the technology employed. Additional data also showed that it is possible to visualize and quantify the fluorescence of the bioactive incorporated using Visia-CR™.

Conclusion: The 3D printing approach employed opens a new perspective in the production of personalized skincare products for different cosmetic applications. Moreover, the possibility to evaluate the bioactive release *in vivo* is being explored.

Keywords: 3D printing; skin patches; personalization; printing settings; *in vivo* performance.

Introduction. The concept of 3D printing comprises a series of processes and technologies, including: powder-based printing (binder jet printing), extrusion-based printing (fused deposition modelling (FDM) and semi-solid extrusion (SSE)), stereolithographic printing (SLA), selective laser sintering printing (SLS), inkjet printing (IJ), and digital light processing (DLP), that can be used as tools to support manufacturing process [1,2]. Thus, it is not surprising that the cosmetics industry is exploring such a versatile technology to innovate its products. In fact, the implementation of 3D printing technologies in the cosmetics industry is opening a new and promising chapter in the development of innovative, cost-effective, sustainable-friendly, personalized and individualized products [2–5]. Furthermore, 3D printing applications are emerging almost daily, and this technology is increasingly penetrating different skincare fields, including the development of customized make-up products (eyeshadows, foundations and mascara brushes), nail art, personalized packaging and individualized hydrogel-based face masks [6].

Focusing on hydrogel-based face masks, SSE-based 3D printing has been explored due to the ability of printing semi-solid 3D constructs using a wide range of polymers with unique properties. This type of technology allows the printing of a product layer-by-layer and, when combined with facial scanning technologies, permits the customization of the product in terms of size and shape, a revolutionizing concept which disrupts the model of one-fits-all [2,7]. Alongside, the adoption of this type of technology can be a solution to innovate the current skincare products available on the market, including the possibility to create products which can also be customized to the costumer, by adjusting features such as pore size, mechanical endurance, and bioactive release profile [2].

However, in the interest of progress, it is important to have full knowledge of print configuration management and construction design, as these can be used as tools for products

personalization [8]. Therefore, the main goal of this work was to develop an innovative and versatile gelatin-based 3D printed patch for multipurpose cosmetic applications, for example anti-aging, that can be easily personalized using a tool that allows the adjustment of the patch's porosity and network topology by changing different print parameters.

Materials and Methods.

Inks Production: Gelatin-based hydrogels were prepared in a water-bath (Nahita International, UK) at 55 ˚C for 1 hour.

3D Printing Process: For the printing tool development, 3-layered patches (20 mm × 20 mm × 0.45 mm) with different infill patterns were printed in an extrusion-based 3D printer (Allevi2, Allevi, USA) employing a 25G nozzle, varying the line distance and the angles to create grid and triangular-shaped pores (Figure 1 (A) and (B)). For each tested condition, measurements of pore area were performed in the ImageJ® software.
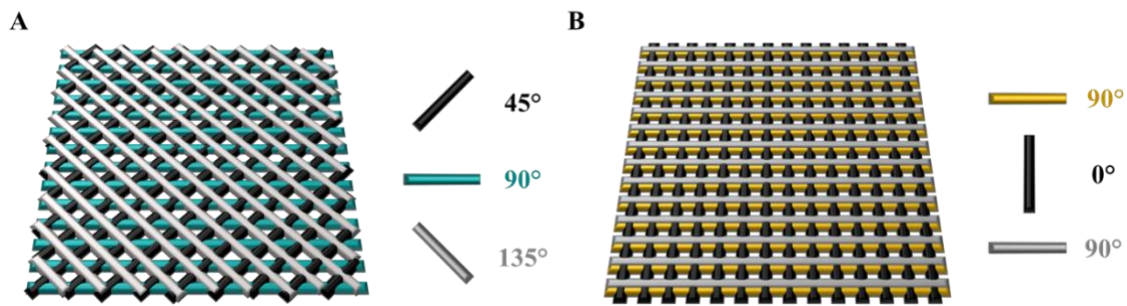

Figure 1. Design and layer orientation. (A) Triangular and, **(B)** grid porous patches.

3D Patches Characterization: First, to validate the possibility of using the Visia-CR™ biometric equipment to record the bioactive fluorescence, IBR-TCLC® in Jojoba Oil 0705 (INCI: *Solanum lycopersicum* Fruit Extract in *Simmondsia chinensis* Seed Oil and Squalene; IBR Lucas Meyer, Israel), which is a fluorescent purified tomato extract rich in colourless carotenoids with recognized antioxidant and anti-aging properties, was incorporated in occlusive patches at concentrations 0.5 to 2.5% to construct a fluorescence calibration curve. Next, IBR-TCLC® triangular-porous patches were printed at the previous defined concentrations, and Visioscan® was used to record the topography through a 3D reconstruction of the printed patches.

Topical application: 1.5% IBR-TCLC®-containing triangular porous patches were applied to the forearm of healthy volunteers (n=2), under occlusion. At these specific time points, a quantitative assessment of the hydration level of the *stratum corneum* (SC) was performed using a Corneometer® CM 825 device. In addition, topographic images were recorded as described above, to understand the application effect on the patch porosity - *in vivo* swelling.

Personalized Eye Patch: Ultimately, Visia-CR™ skin analysis imaging system was employed as a 2D skin scanner for designing a personalized eye patch with controlled network topology; the patch was customized to the volunteer face measurements on the *onshape* CAD software.

Results. The 3D printing data showed that it is possible to produce gelatin-based hydrogel patches with different degrees of porosity by varying the printing settings, such as line distance and printing angle. The average pore area in patches with grid format was notoriously influenced by the distance between filaments, decreasing with the decrease in line distance. Specifically, by varying the line distance from 1.6 to 0.7 mm, pore area values of 0.821 ± 0.017 mm^2 (1.6 mm), 0.315 ± 0.007 mm^2 (1.3 mm) and 0.060 ± 0.010 mm^2 (0.7 mm) were obtained. Regarding printing accuracy, the patches with line distances of 1.6 and 1.3 mm showed consistent pore area values throughout the whole pool, with an adequate overlaying of intercalated filaments. In the patch with a line distance of 0.7 mm, the pore areas were relatively inconsistent, which suggests that 0.7 mm is the maximum distance that can be defined for the type of nozzle employed (25G, inner diameter = 0.280 mm), to guarantee printing accuracy and precision. By varying the printing angle, it was possible to create both triangular and grid pores using an equal line distance of 1.3 mm. The results show that, although the printing angle is varied, it is possible to obtain pores with similar areas: patch 45°-90°-135° (0.312 ± 0.058 mm^2), patch 25°-155°-25° (0.344 ± 0.012 mm^2) and patch 45°-135°-45° (0.341 ± 0.009 mm^2).

As a proof-of-concept, the anti-aging bioactive IBR-TCLC® was incorporated into the gelatin-based formulation ink at different concentrations. First, to test the sensitivity of the equipment - Visia-CR™, to visualize and record the fluorescence of the bioactive incorporated, images of occlusive patches with different IBR-TCLC® concentrations were recorded, as shown in Figure 2 (A). The results show that it is possible to distinguish the

different fluorescence intensities of the samples. For quantification purposes, the data obtained was used to build a calibration curve, with the equation: $y = 22.037x + 153.46$ ($R^2 = 0.9871$) – Figure 2 (B). Afterwards, IBR-TCLC® (0.5 to 2.5%)-containing triangular patches were printed (Figure 2 (C)), and the topographic analysis showed that the incorporation of IBR-TCLC® did not significantly affect the printing accuracy and pore shape fidelity, i.e., patches with different concentrations of IBR-TCLC® had a porosity degree similar to that of the gelatin-based control.
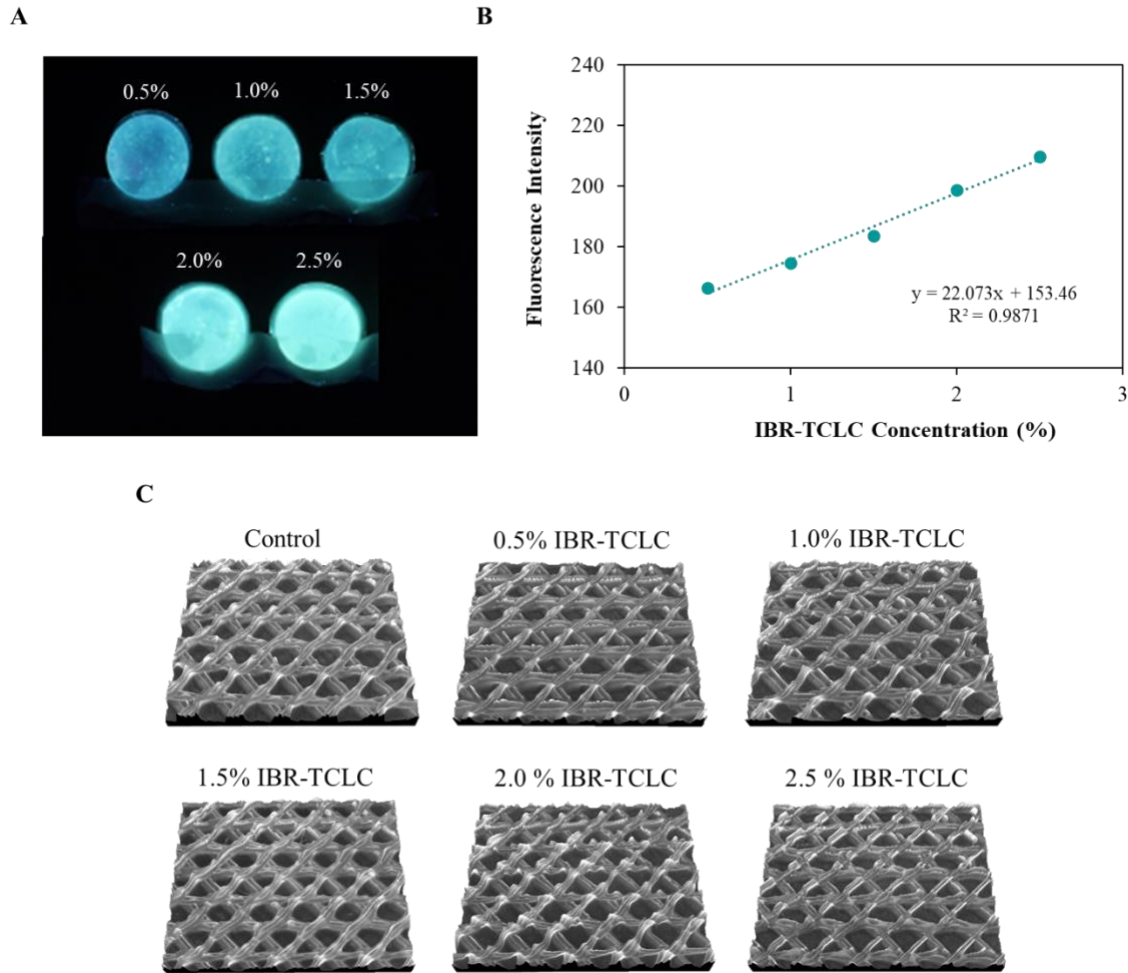

Figure 2. Gelatin-based patches with different concentrations of IBR-TCLC®. **(A)** Visualization of the fluorescence intensity of occlusive patches on Visia-CR™. **(B)** Fluorescence calibration curve. (**C**) 3D reconstruction of porous printed patches - topographic analysis.

As for the topical application of the IBR-TCLC® porous patches (Figure 3 (A)), it was possible to infer that after 24 hours of application there was a significant swelling of the vehicle (closer pores) – Figure 3 (B). Furthermore, hydration data show that the patches application increased the moisture content in 39.91% (t_0h = 35.9 ± 1.59 and t_24h = 50.23 ± 3.48).
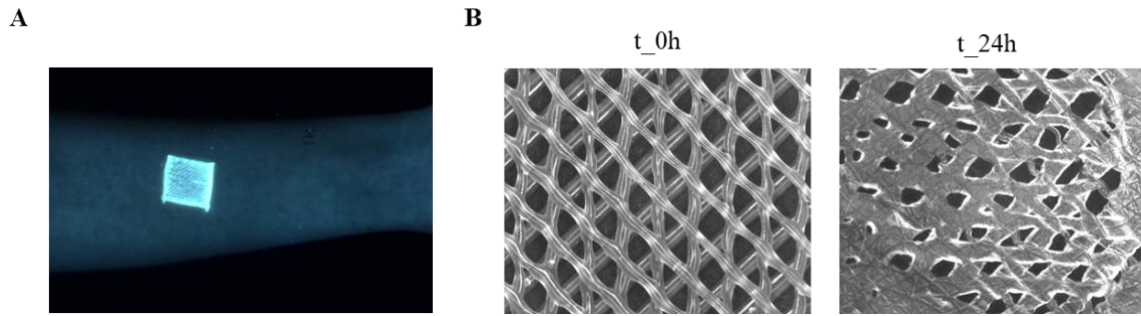

Figure 3. Topical application of the 3D printed gelatin-based porous patches containing 1.5% IBR-TCLC®. (A) Visualization of patch fluorescence when applied to the forearm of a volunteer. **(B)** Patch topography before (t_0h) and after application (t_24h).

Afterwards, the structures were evolved to produce more complex, effective and customized forms, to meet the current market needs. Thus, a personalized eye patch with controlled network topology was designed and printed considering the 2D anatomy of a selected volunteer (Figure 4 (A) and (B)). The results presented in Figure 4 (C) and (D) show that it is possible to increase the complexity levels of the structures, without changing the printing conditions (i.e., pressure, line distance and layer height), which attests to the versatility of the formulation developed.
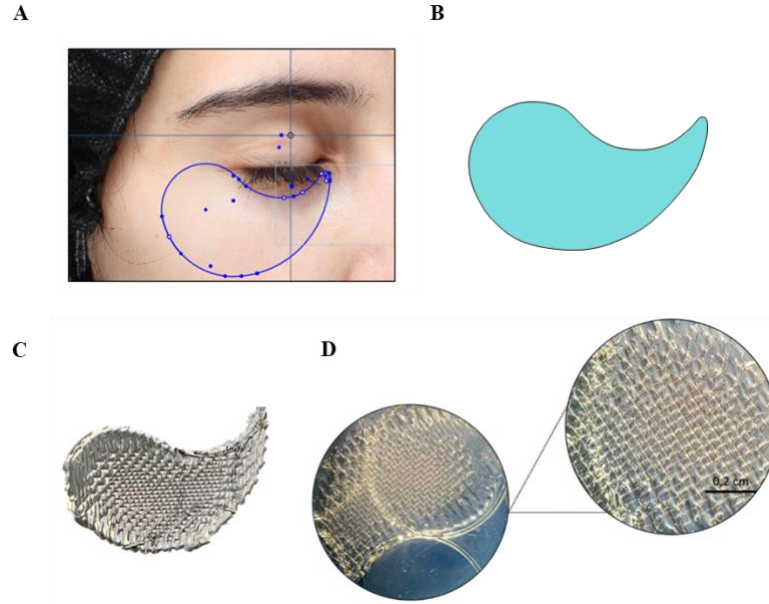
Figure 4. IBR-TLCL® gelatin-based personalized eye patch. (A) Sketch of the patch drawn in a personalized pattern on top of a face captured by a high-resolution camera and Visia-CR™. **(B)** Eye patch designed in *onshape* CAD software. **(C)** Final printed eye patch. **(D)** Visualization of the porosity degree.

Discussion. The obtained pore width measurements were used to establish a tool that allows personalizing the internal geometry of the printed patches, controlling the pore size, which greatly impacts the patch performance and applicability. For example, specifying a smaller distance between filaments will lead to the printing of more compact and denser patches [9], which may slow down the release of bioactives, while the orientation of the filaments will influence the resistance of the vehicle [10]. Hence, it is essential to understand the influence of the most relevant printing parameters, that can be used to quickly adjust the design of the patches to the customer needs. The data obtained showed that it is possible to create patches with different internal geometries (namely, grid and triangular pores) and porosity levels, by varying the line distance and printing angle. Furthermore, the range of pore areas obtained herein agrees with those reported in other studies [9,11], which highlights the importance of this type of research by emphasizing that it is possible to achieve similar pore-related features when using distinct formulations and printing conditions, possibly overcoming design-related incompatibilities that can sometimes hinder the rapid personalization of the printed patches. Furthermore, the porosity data obtained also suggest that it is possible to vary the

7

printing angle (from 90° to 45° and 25°) and maintain identical porosity levels for equal distances between filaments. This reinforces the relevance of employing adequate printing optimization strategies, since it is well stablished that acute angles ($0° < \alpha < 90°$) are prone to higher filament deposition due to closer path lengths, when compared to right ($\alpha = 90°$) and obtuse angles ($90° < \alpha < 180°$) [12,13].

The characterization studies show that it is possible to distinguish and quantify the fluorescence of the incorporated substance. Furthermore, the topographic results indicate that the incorporation of different concentrations of IBR-TCLC® does not significantly affect the printing accuracy and pore shape fidelity, which reinforces the versatility of the developed gelatin-based formulation and of the used technology.

In terms of topical application, a significant swelling of the patch was observed, which can be advantageous to modulate and control the bioactive release. Furthermore, its application has been shown to promote the skin hydration. To understand the influence of the patch porosity on the treatment outcome, patches with different degrees of porosity are being tested in ongoing *in vivo* studies. Moreover, the possibility to evaluate the bioactive release *in vivo* is being explored.

Finally, in this work we also pursued customization of the size and shape of the patches. This personalization step is crucial due to the huge variation in people's face shapes and on the location, size, and shape of their features. The data obtained highlights the relevance of coupling facial scanning technologies to the printing process, allowing the design and printing of patches that anatomically fit the consumer face.

Conclusion. This work provided insight over the practicality of employing 3D printing for the production of versatile personalized skin care products with reproducible and controlled pore geometries, which may represent an opportunity in terms of modulating the bioactive release. Such scenario offers a great versatility to this kind of vehicle, which can be quickly modified to adjust to the different requirements of different skins. Furthermore, these data can provide a baseline from which to evolve towards the printing of advanced structures that perfectly fit the face of each consumer and that can incorporate, for example, different

bioactive concentrations and/or porosity levels within the same framework, thus improving the personalization of skincare products.

Conflict of Interest Statement. All the authors declare no conflict of interest.

References.

[1]   S. Bom, C. Santos, R. Barros, A.M. Martins, P. Paradiso, R. Cláudio, P.C. Pinto, H.M. Ribeiro, J. Marto, Effects of starch incorporation on the physicochemical properties and release kinetics of alginate-based 3D hydrogel patches for topical delivery, Pharmaceutics. 12 (2020) 1–20. https://doi.org/10.3390/pharmaceutics12080719.

[2]   S. Bom, A.M. Martins, H.M. Ribeiro, J. Marto, Diving into 3D (bio)printing: A revolutionary tool to customize the production of drug and cell-based systems for skin delivery, Int. J. Pharm. 605 (2021) 1–20. https://doi.org/10.1016/j.ijpharm.2021.120794.

[3]   J. Goole, K. Amighi, 3D printing in pharmaceutics: A new tool for designing customized drug delivery systems, Int. J. Pharm. 499 (2016) 376–394. https://doi.org/10.1016/j.ijpharm.2015.12.071.

[4]   Z. Liu, Q. Jiang, Y. Zhang, T. Li, H.C. Zhang, Sustainability of 3D printing: A critical review and recommendations, in: ASME 2016 11th Int. Manuf. Sci. Eng. Conf., 2016: pp. 1–8. https://doi.org/10.1115/MSEC2016-8618.

[5]   J. Norman, R.D. Madurawe, C.M.V. Moore, M.A. Khan, A. Khairuzzaman, A new chapter in pharmaceutical manufacturing: 3D-printed drug products, Adv. Drug Deliv. Rev. 108 (2017) 39–50. https://doi.org/10.1016/j.addr.2016.03.001.

[6]   N.P. Kim, J. Kim, M.S. Han, The convergence of three-dimensional printing and nail-art technology, J. Cosmet. Med. 3 (2019) 94–101. https://doi.org/10.25056/jcm.2019.3.2.94.

[7]   A. Goyanes, U. Det-Amornrat, J. Wang, A.W. Basit, S. Gaisford, 3D scanning and 3D

printing as innovative technologies for fabricating personalized topical drug delivery systems, J. Control. Release. 234 (2016) 41–48. https://doi.org/10.1016/j.jconrel.2016.05.034.

[8]   S. Bom, R. Ribeiro, H.M. Ribeiro, C. Santos, J. Marto, On the progress of hydrogel-based 3D printing: Correlating rheological properties with printing behaviour, Int. J. Pharm. 615 (2022) 1–14. https://doi.org/10.1016/j.ijpharm.2022.121506.

[9]   L. Tytgat, M.R. Kollert, L. Van Damme, H. Thienpont, H. Ottevaere, G.N. Duda, S. Geissler, P. Dubruel, S. Van Vlierberghe, T.H. Qazi, Evaluation of 3D Printed Gelatin-Based Scaffolds with Varying Pore Size for MSC-Based Adipose Tissue Engineering, Macromol. Biosci. 20 (2020) 1–6. https://doi.org/10.1002/mabi.201900364.

[10]   H. Zhao, J. Xu, H. Yuan, E. Zhang, N. Dai, Z. Gao, Y. Huang, F. Lv, L. Liu, Q. Gu, S. Wang, 3D printing of artificial skin patches with bioactive and optically active polymer materials for anti-infection and augmenting wound repair, Mater. Horizons. 9 (2022) 342–349. https://doi.org/10.1039/d1mh00508a.

[11]   T. Kreller, T. Distler, S. Heid, S. Gerth, R. Detsch, A.R. Boccaccini, Physico-chemical modification of gelatine for the improvement of 3D printability of oxidized alginate-gelatine hydrogels towards cartilage tissue engineering, Mater. Des. 208 (2021) 109877. https://doi.org/10.1016/J.MATDES.2021.109877.

[12]   S. Naghieh, M.D. Sarker, N.K. Sharma, Z. Barhoumi, X. Chen, Printability of 3D printed hydrogel scaffolds: Influence of hydrogel composition and printing parameters, Appl. Sci. 10 (2019) 1–18. https://doi.org/10.3390/app10010292.

[13]   Y. He, F. Yang, H. Zhao, Q. Gao, B. Xia, J. Fu, Research on the printability of hydrogels in 3D bioprinting, Sci. Rep. 6 (2016) 1–13. https://doi.org/10.1038/srep29977.